Published online 28 February 2013 *Nucleic Acids Research, 2013, Vol. 41, No. 7* ***4065–4079***
doi:10.1093/nar/gkt131

Human SIRT1 regulates DNA binding and stability of the Mcm10 DNA replication factor via deacetylation

Samuel T. Fatoba[1], Silvia Tognetti[1], Melissa Berto[1], Elisabetta Leo[1,2], Claire M. Mulvey[3], Jasminka Godovac-Zimmermann[3], Yves Pommier[2] and Andrei L. Okorokov[1,*]

[1]Wolfson Institute for Biomedical Research, University College London, Gower Street, London WC1E 6BT, UK, [2]Laboratory of Molecular Pharmacology, Center for Cancer Research, National Cancer Institute, National Institutes of Health, 37 Convent Drive, Bethesda, MD 20892-4255, USA and [3]Proteomics and Molecular Cell Dynamics, University College London, Royal Free Campus, Rowland Hill Street, London NW3 2PF, UK

Received September 17, 2012; Revised February 7, 2013; Accepted February 9, 2013

ABSTRACT

The eukaryotic DNA replication initiation factor Mcm10 is essential for both replisome assembly and function. Human Mcm10 has two DNA-binding domains, the conserved internal domain (ID) and the C-terminal domain (CTD), which is specific to metazoans. SIRT1 is a nicotinamide adenine dinucleotide (NAD)-dependent deacetylase that belongs to the sirtuin family. It is conserved from yeast to human and participates in cellular controls of metabolism, longevity, gene expression and genomic stability. Here we report that human Mcm10 is an acetylated protein regulated by SIRT1, which binds and deacetylates Mcm10 both *in vivo* and *in vitro*, and modulates Mcm10 stability and ability to bind DNA. Mcm10 and SIRT1 appear to act synergistically for DNA replication fork initiation. Furthermore, we show that the two DNA-binding domains of Mcm10 are modulated in distinct fashion by acetylation/deacetylation, suggesting an integrated regulation mechanism. Overall, our study highlights the importance of protein acetylation for DNA replication initiation and progression, and suggests that SIRT1 may mediate a crosstalk between cellular circuits controlling metabolism and DNA synthesis.

INTRODUCTION

Eukaryotic cells initiate DNA replication from multiple origins that are scattered along the chromosomes. The initiation of chromosomal DNA replication is a convergence point for signalling pathways co-ordinating cellular proliferation (1–4). The activation of replication origins is a two-step mechanism that begins with the ordered formation of a macromolecular protein complex referred to as the pre-replicative complex (preRC) during late mitosis and early G1 (1–4). At this stage, replication origins are bound by the origin recognition complex (ORC), which serves as a platform for sequential assembly of the initiator proteins Cdc6, Cdt1 and Mcm2–7 into preRCs in a process commonly known as 'origin licensing'. The second step is dependent on the activation of cyclin-dependent kinases and the Cdc7/Dbf4 kinase complex, which promote the transition from preRCs to pre-initiation complexes in a temporally regulated manner throughout S phase. This step, also referred to as 'origin firing', involves the recruitment to origins of Mcm10, Cdc45 and additional initiator proteins that collectively are capable of promoting DNA origin unwinding and recruiting DNA polymerases (1–4).

Current research in yeast and metazoans has clearly demonstrated that Mcm10 is essential for DNA replication initiation (1–4). The human replication initiation factor Mcm10 is a multifunctional protein that interacts with DNA and replisome protein components (5–15). Free Mcm10 has also been reported to stabilize DNA polymerase α-primase by formation of a soluble complex, which in co-operation with And1/Ctf4 complex is then targeted to origins (16,17). Human Mcm10 has two DNA-binding domains: the conserved internal domain (ID) and the C-terminal domain (CTD, specific to metazoans), both capable of binding single-stranded DNA (ssDNA) (18–21). After replication initiation, Mcm10 remains associated with the migrating DNA replication fork and

*To whom correspondence should be addressed. Tel: +44 20 7679 0959; Fax: +44 20 7209 0470; Email: a.okorokov@ucl.ac.uk
Present address:
Claire M. Mulvey, Department of Biochemistry, Cambridge Centre for Proteomics, University of Cambridge, Tennis Court Road, Cambridge CB2 1QR, UK.

The authors wish it to be known that, in their opinion, the first two authors should be regarded as joint First Authors.

inactivation or depletion of Mcm10 inhibits S-phase progression (22). Mcm10-knockdown cells exhibit slower early and mid, and aberrantly late, S-phase DNA replication (23). Prolonged Mcm10 depletion leads to Chk1-dependent DNA damage response and subsequent apoptosis (24). Human Mcm10 forms a hexameric ring that appears to serve as a docking module between critical replication factors necessary for origin firing (10). However, apart from reports on cell cycle-dependent phosphorylation of Mcm10 (8,13) and on the requirement of di-ubiquitination for binding to PCNA protein (25), little is known about the functional regulation of Mcm10.

Acetylation of proteins appears to be one of the most conserved post-translational modifications across all life domains, and its counterbalance by deacetylation is now accepted as a common regulatory event in the modulation of stress response, transcription activation and enzymatic activity, chromatin structure, DNA repair and stability of many proteins (26–29). SIRT1 is a human homologue of yeast Sir2. It belongs to the family of sirtuins that are conserved from yeast to human. SIRT1 is a class III histone deacetylase (HDAC) that catalyses the removal of acetyl moiety from the ε-amino groups of conserved lysine residues in histones in nicotinamide adenine dinucleotide (NAD)-dependent manner (30,31). The seven human sirtuins differ in their subcellular localization. SIRT1, SIRT6 and SIRT7 are predominantly nuclear, whereas SIRT2 is mainly cytoplasmic, though it can be shuttled to the nucleus during mitosis (32,33). SIRT3, SIRT4 and SIRT5 are located in mitochondria. SIRT1 has been implicated in the control of chromatin structure, transcription and DNA repair, serving as a crucial link between cell metabolism, control of genomic stability, longevity and aging (30,31,34,35). Sir2 has been shown to negatively regulate a subset of DNA replication origins (~20%) in *Schizosaccharomyces pombe* by affecting preRC assembly (36–38). Sir2 in *Saccharomyces cerevisiae* has also been implicated in controlling the timing of replication origins by reprogramming them from early to late (39). Although protein interactions between Mcm10 and Sir2 have been reported in yeast, their significance remains unexplored in human cells (40–42). In humans, SIRT1-dependent deacetylation has been reported to modulate the DNA-binding properties of important proteins that are regulated by acetylation/deacetylation. The list of SIRT1 targets includes the transcription factors p53, E2F1, FOXO1 and FOXO3a, and the DNA repair proteins Ku70, WRN, NBS and XPA (43–48).

In this study, we explored the interactions between Mcm10 and SIRT1 in human cells and their functional implications. We demonstrate that (i) Mcm10 is an acetylated protein and (ii) SIRT1 interacts directly with Mcm10 and modulates its DNA binding and stability via deacetylation. This novel regulatory mechanism suggests that, like transcription and DNA repair factors, human DNA replication proteins are also modulated by acetylation/deacetylation and this could be important during assembly, initiation and function of the replisome.

MATERIALS AND METHODS

Recombinant DNA plasmids and proteins

Plasmids coding for Flag-SIRT1 (pCDNA3.1-Flag-hSIRT1) and GST-SIRT1 (pGEX-5X-hSIRT1) were obtained from Prof. Fuyuki Ishikawa and Dr. Nobuyuki Tanimura (Kyoto University, Japan). pCDNA3.1-p300 (49) and pCDNA3.1-vectors coding for Flag-SIRT2, SIRT5, SIRT6 and SIRT7 (50) were all obtained from Addgene, with Addgene plasmid numbers 23252, 13813, 13818, 13817, 13818, respectively. SIRT2, SIRT5, SIRT6 and SIRT7 cDNAs were used to subclone into pGEX-6P1 and pGEX-6P3 vectors to generate GST fused SIRT2, 5, 6 and 7.

Full length (FL) of Mcm10 was expressed similar to the previously described (10). N-terminal domain (NTD) (aa 1–223), ID (aa 224–466) and CTD (aa 630–874) of Mcm10 were subcloned into pProEX-HT-B expression vector (Invitrogen). Expression of H_6-Mcm10 protein and its domains was induced with 1 mM Isopropyl β-D-1-thiogalactopyranoside (IPTG) in *Escherichia coli* strain Rosetta (Novagen) for 12 h at 15°C. Cells were lysed in 25 mM Tris–HCl, pH 9.0, 500 mM NaCl, 10 mM $MgCl_2$, 25 mM KCl, 10% glycerol. The proteins were isolated by Ni^{++} metal affinity chromatography, eluted with 25 mM Tris–HCl, pH 7.5, 150 mM NaCl, 10 mM $MgCl_2$, 25 mM KCl buffer containing 250 mM imidazole and further purified by gel filtration, aliquoted, flash-frozen in liquid nitrogen and stored at −80°C. Commercial preparates of SIRT1 and p300 HAT were obtained from BioMol (ENZO Life Science). Acetyl-CoA (AcoA), NAD and NIA were all obtained from Sigma.

Cell cultures, transfections and siRNA

HCT116 cells were cultivated in McCoy 5A growth medium (GIBCO) supplemented with 10% foetal bovine serum (FBS) and antibiotics (penicillin/streptomycin). Plasmid DNA was transfected using Lipofectamine™ 2000 (Invitrogen) according to manufacturer's instruction. For RNA interference (RNAi), non-targeting small interfering RNA (siRNA) (siRNA #1) and SIRT1 siRNA were obtained from Dharmacon, while Mcm10 siRNA was obtained from Applied Biosystems. Exponentially growing cells in a six-well plate format were transfected with siRNA complex prepared in OptiMEM (Invitrogen) and transfected using Lipofectamine™ RNAiMAX (Invitrogen) according to manufacturer's instructions. Cells were incubated for additional 48 h (unless stated otherwise) and the silencing of proteins was confirmed by western blot (WB). SIRT1-siRNA sequence was 5′-ACUUUGCUGUAACC CUGUA-3′ and Mcm10-siRNA sequence was 5′-CGGCG ACGGUGAAUCUUAU-3′.

Cell synchronization and extract fractionation

Cells were grown to 40% of confluence in six-well plates, changed into medium containing 2 mM thymidine and incubated for further 24 h, after which they were washed with phosphate buffered saline (PBS) containing 2 mM thymidine, transfected with anti-SIRT1 or control

siRNA and further incubation in Mc-Coy medium containing 2 mM thymidine without antibiotics. Twenty-four hours post-transfection cells were washed once with 2 ml of PBS plus 2 mM thymidine and placed into fresh Mc-Coy medium with 10% FBS, 1% antibiotics and 2 mM thymidine. After further 12 h, cells were washed with PBS and incubated in thymidine-less McCoy medium with 10% FBS and antibiotics. Cells then were harvested at different time points following the release from the thymidine block. At those points, cells were harvested, washed with PBS and centrifugated (1400 rpm, 4°C, for 2 min). After discarding supernatant, cell pellet was resuspended in 200 µl of Buffer A [10 mM 4-(2-hydroxyethyl)-1-piperazineethanesulfonic acid (HEPES), pH 7.9, 10 mM KCl, 1.5 mM $MgCl_2$, 0.34 M sucrose, 10% glycerol, 1 mM dithiothreitol (DTT), 0.1% Triton X-100, protease inhibitor cocktail (Roche)] and incubated on ice for 8 min. After that, samples were centrifuged at 3700 rpm, 4°C, for 5 min. The supernatant was separated into the fractions S1 (cytoplasmic fraction) and pellet fraction P1 (nuclear fraction). Fraction S1 was then further clarified by centrifugation at 13 200 rpm, 4°C, for 5 min and its supernatant was collected into the S2 fraction, which contained soluble cytoplasmic protein. Fraction P1 was washed once with 200 µl of Buffer A and resuspended by pipetting in 150 µl of Buffer B [3 mM ethylenediaminetetraacetic acid (EDTA), 0.2 mM ethylene glycol tetraacetic acid (EGTA), 1 mM DTT, protease inhibitor cocktail (Roche)]. The fraction then was further incubated for 30 min on ice and centrifuged at 4300 rpm, 4°C, for 5 min. Separated supernatant (fraction S3) contained nuclear soluble proteins and the pellet (fraction P3) contained chromatin. Pellet (P3) was washed once with 150 µl of Buffer B and resuspended in 80 µl of Buffer B plus 0.5 µl of the Benzonase enzyme (Novagen), and samples were incubated at room temperature for 15 min. Samples were then aliquoted, flash-frozen in liquid nitrogen, stored at −80°C, and used for further analysis.

Immunoprecipitation and western blot analysis

Samples were prepared for immunoblotting by lysis in Radio-Immunoprecipitation Assay buffer (RIPA) buffer [0.1% sodium dodecyl sulphate (SDS), 50 mM Tris-HCl (pH 7.5), 1% sodium deoxycholate, 1% nonyl phenoxypolyethoxylethanol (NP-40), 1 mM EDTA, protease inhibitor cocktail (Roche), (150 mM NaCl or 300 mM NaCl, low or high stringency, respectively)]. For immunoprecipitation (IP), clarified RIPA cell lysates were incubated with relevant primary antibody overnight at 4°C. The resultant immunocomplexes were precipitated by incubation with Protein A sepharose (GE Healthcare). After sufficient wash, samples were analysed by WB. Samples were resolved on 4–12% 3-(N-morpholino)propanesulfonic acid (MOPS) gels (Invitrogen) and transferred onto nitrocellulose membrane with a semidry apparatus for 1 h at 15 V. Membrane was blocked in PBS containing 10% milk and 0.2% Tween-20 and probed with the required antibodies.

Mcm10 antibody was raised in rabbit against N-terminus (1–279 aa) of Mcm10 and immunopurified (Eurogentec), whereas the other antibodies were purchased from commercial sources as indicated. SIRT1 antibody (Santa Cruz biotechnology, USA), anti-Flag (Sigma), γH2AX (Upstate); anti-α-tubulin, His-tag, GST-tag, acetyl-lysine (K-Ac), H3K9-Ac and histone H3 antibodies were all purchased from Abcam. Antibody signals were detected with ECL Chemiluminescent Substrate (Pierce). Anti-mouse and anti-rabbit secondary antibodies were from (Dako Denmark A/S).

Molecular combing

Forty-eight hours after transfection with siRNA, HCT116 cells were pulse labelled for 20 min with 100 µM IdU (Sigma), quickly washed with PBS and pulse labelled for another 20 min with 100 µM CldU (Sigma). Cells were then trypsinized, embedded in low melting agarose plugs and treated as described (51,52). Briefly, after cell lysis and agarose digestion, DNA fibers were combed on silanized coverslips, denatured with NaOH and replicons were detected with anti-IdU and anti-CldU antibodies. Images of replicated DNA were captured using the epi-fluorescence microscope Pathway (Becton Dickinson) with Attovision software. Signals were measured using ImageJ (NCI, NIH) with custom-made modifications. For the calculation of fork velocities, only replicons with signals that had similar length for IdU and CldU were considered, to exclude the possibility of broken or arrested forks. If not specified, a minimum number of 200 replicons were analysed to generate each histogram for fork velocities, and 50 couples of adjacent replicons for the inter-origin distances.

GST pull-down assay

GST and GST-tagged sirtuin proteins were expressed and purified from bacteria using standard methods. Equimolar quantities of purified proteins were conjugated to glutathione-Sepharose beads and incubated with different purified Mcm10 domains. Beads were incubated for 1 h at +4°C with rotation, washed extensively, then 50 µl of loading buffer (3×) containing DTT to reduce disulphide bonds and SDS were added to the samples. The samples were boiled at 95°C for 5 min and analysed using 4–12% MOPS gels (Invitrogen) followed by WB with either anti-His or anti-GST antibodies. Bound Mcm10 protein was quantified relative to SIRTs input using densitometry (AlphaEase FC software).

In vitro acetylation and deacetylation assays

In vitro acetylation assays were set as advised by the manufacturer of recombinant p300 HAT (BioMol, ENZO Life Science) and as described in (53). Briefly, target proteins (1 µg of NTD, ID, CTD or 3 µg of Mcm10 FL were incubated for 60 min at 30°C with AcoA (final 0.33 mM) and 0.5 µg of p300 HAT (5.7 µ/mg). SIRT1-dependent deacetylation assays reactions were set as advised by the manufacturer of SIRT1 (BioMol, ENZO Life Sciencev). Subsequent deacetylation assays were started as described above to acetylate protein

substrates for 1 h at 30°C, then 0.5 μg of commercial SIRT1 (BioMol, ENZO Life Science) or 1 μg of GST-SIRT1 and 1 mM of NAD and incubated for further 45 min at 30°C. Deacetylation reactions were blocked by addition of NIA to 50 mM final concentration. All reactions were stopped by boiling at 95°C for 5 min and analysed using 4–12% MOPS gels (Invitrogen) followed by WB with anti-K-Ac antibody.

Mass spectrometry

Following *in vitro* (de)acetylation assays, recombinant Mcm10 protein products (ID and CTD) were each separated by SDS polyacrylamide gel electrophoresis and visualized by silver-staining (ProteoSilver Plus, Sigma Aldrich, Poole, UK). Bands corresponding to the correct molecular weight for each product were excised from the gel, destained and processed with the Progest Investigator instrument (Digilab, Huntingdon, UK) using established protocols for reduction and alkylation (54). Gel plugs were rehydrated in 20 μg/ml sequencing grade modified trypsin (Promega, Southampton, UK) and incubated overnight at 37°C. Tryptic peptides were eluted, vacuum-dried, resuspended in 0.1% formic acid and analysed by liquid-chromatography mass spectrometry performed with an LTQ-Orbitrap Classic mass spectrometer (Thermo Fisher Scientific, UK). Details of mass spectrometry and subsequent data analysis can be found in Supplementary Methods.

Electromobility shift assay

Sixty-nucleotide long ssDNA: 5′-TGCCAAGCTTGCATGCCTGCAGGTCGACTCTAGAGG-3′ was used for band shift experiments. The DNA was 5′-labelled with ^{33}[P] using T4 Polynucleotide Kinase (Promega) and [γ-^{33}P]ATP for 1 h at 36°C. Labelled DNA was purified with ''NTP wash'' kit Qiagen and the DNA has been checked on 20% TBE gel run in 1× TBE at 160 V. DNA-binding properties of Mcm10 and its acetylated/deacetylated domains were studied by electrophoretic mobility shift assay. The final volume of DNA-binding mixtures was 20 μl, of which the DNA template was typically 4 μl (20 μg/ml) and the remaining volume was made of the protein sample (NTD 1 μg, ID 1 μg, CTD 1 μg, FL 0.5 μg, SIRT1 1 μg or p300 0.5 μg) and the reaction buffer (25 mM Tris–HCl, pH 8.0, 2 mM DTT, 50 mM NaCl, 2.5 mM of $MgCl_2$). Whenever p300 and/or SIRT1 were present, reactions were supplemented with AcoA and/or NAD^+, respectively.

The reactions were incubated for 10 min at room temperature when direct protein–DNA interaction was tested, 60 min at 36°C when acetylated Mcm10 proteins were tested and further 40 min at 36°C when an additional incubation with SIRT1 took place. All samples were kept for 20 min on ice before loading onto 6% 0.5× TBE Novex DNA Retardation gels (Invitrogen). A volume of 5 μl of 6× DNA loading buffer (Promega) was added before loading the samples onto 6% 0.5× TBE Novex DNA Retardation gels (Invitrogen). After running at 90 V in 0.5× TBE at 4°C, gels were dried and analysed by autoradiography. The radioautography images obtained after exposure were scanned and densitometric analysis of the protein-shifted DNA bands was performed using AlphaEasePC software.

Flow cytometry (FACS) analysis

Before harvesting cells, BrdU was added to a final concentration of 10 μM for 1 h. Cells were then collected, washed with PBS containing 3% bovine serum albumin and prepared for analysis using the APC BrdU flow kit (BD Pharmingen^{TM}) according to manufacturer's procedure. The stained cells were analysed for total DNA (7AAD incorporation) and BrdU incorporation using the FlowCyan ADP machine (Becton Dickinson). Data were analysed with the Summit 4.3 software.

RESULTS

Human Mcm10 specifically interacts with SIRT1 *in vivo*

To determine whether human Mcm10 and sirtuin proteins specifically interact with each other, we tested Mcm10's interaction with SIRT1, SIRT2, SIRT5, SIRT6 and SIRT7. SIRT1 and SIRT2 have been reported the most robust deacetylases (50,55). We transiently expressed Mcm10 in combination with each of these different sirtuins in human cells. All sirtuins were Flag-tagged to allow their precipitation, whereas Mcm10 was immunoprecipitated by polyclonal anti-Mcm10 antibody. Mcm10-SIRTs complexes formed *in vivo* were isolated by IP with either anti-Mcm10 or anti-Flag antibodies, and complexes were analysed by immunoblotting (Figure 1A and B).

As shown in Figure 1A (left panel), Flag-SIRT1 was the only SIRT that efficiently co-precipitated with Mcm10. Conversely, for the five different SIRTs tested, Mcm10 was only co-precipitated with Flag-SIRT1 (Figure 1B, top panel), indicating that Mcm10 specifically interacts with SIRT1. The SIRT1–Mcm10 interaction was highly specific, as none of the other sirtuins (SIRT2, SIRT5, SIRT6 and SIRT7) was efficiently co-precipitated with Mcm10 under the same conditions (Figure 1A and B).

SIRT1 interacts with the C-terminus of Mcm10

We next analysed whether the SIRT1–Mcm10 interaction was direct using recombinant GST-tagged sirtuins *in vitro* (Figure 1C). Recombinant Mcm10 was found to bind specifically to SIRT1. Only SIRT6 among the other sirtuins showed some low-level interaction with Mcm10 (Figure 1C*i* and *ii*).

Further analysis of Mcm10 derivatives showed that SIRT1 selectively strongly interacted with the CTD of Mcm10 (residues: 636–874), the domain which is specific to metazoan Mcm10 and absent in the yeast protein ortholog (Figure 1D). This CTD has two additional Zn-finger motifs located at the C-terminal end and has been reported to bind ssDNA (16,17). We therefore tested whether these Zn-finger motifs were required for SIRT1–Mcm10 association and whether the presence of ssDNA would affect their interaction. As shown in Figure 1E, neither EDTA nor ssDNA affected SIRT1–Mcm10

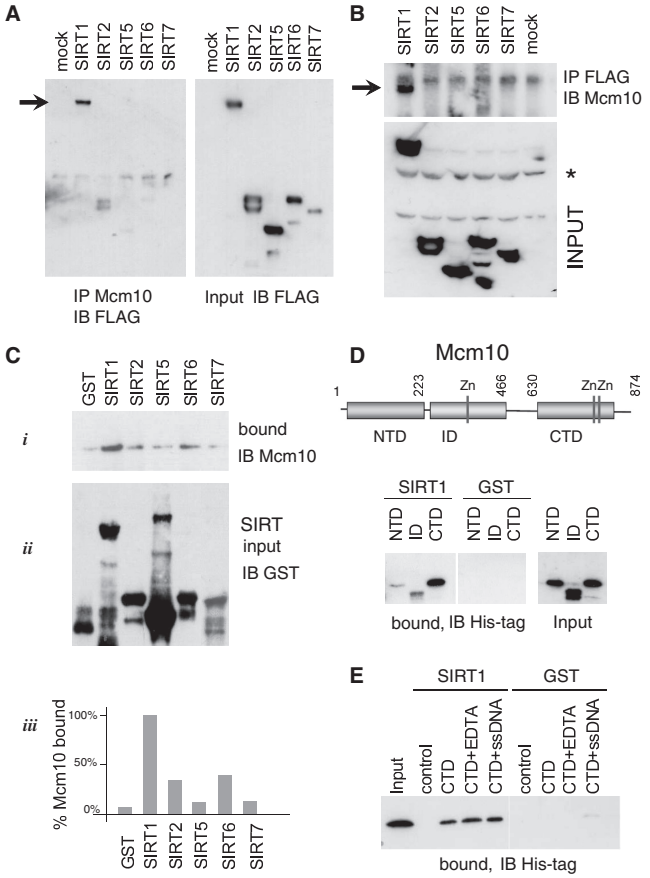

Figure 1. SIRT1 interacts with Mcm10 *in vivo* and *in vitro*. (**A** and **B**) HCT116 cells were co-transfected with plasmids (3 μg each) encoding His-tagged Mcm10 and Flag-tagged sirtuins. Anti-Mcm10 and anti-Flag immunoprecipitates (IP) were analysed by WB with the indicated antibodies. Co-immunoprecipitations indicated that Mcm10 interaction was specific to SIRT1. Arrows indicate SIRT1 on left panel in A, and Mcm10 on the top panel in B. (B) Input panel shows signals obtained with both anti-Mcm10 and anti-Flag antibodies. Mcm10 is indicated with asterisk. (**C**) GST-fused sirtuin proteins coupled to Sepharose beads were incubated with recombinant Mcm10. After beads were washed, bound proteins were analysed by WB with anti-Mcm10 antibody (*i*). The input proteins were analysed with anti-GST antibody (*ii*), and the relative binding of sirtuins to Mcm10 was compared with SIRT1 (*iii*). (**D**) GST-fused SIRT1 bound to Sepharose beads was incubated with different His-tagged deletion mutants of Mcm10, which represented its separate NTD, ID and CTD. SIRT1 interacting Mcm10 domains were identified by WB with anti-His antibody. Strong and weak interactions were observed for CTD and ID, respectively. (**E**) Sepharose beads with bound GST-SIRT1 were incubated with Mcm10 CTD in the presence of either EDTA or ssDNA (60 nt). Neither condition affected Mcm10 interaction with SIRT1.

complex formation, indicating that the interaction between these two proteins requires an epitope different from Zn-finger motifs and can potentially take place when Mcm10 is bound to DNA.

Mcm10 is an acetylated protein and is deacetylated by SIRT1 *in vivo*

The interaction between Mcm10 and SIRT1 suggested that Mcm10 could be a substrate for SIRT1 deacetylase activity. To test this hypothesis, we first determined whether Mcm10 is acetylated *in vivo*. As shown in Figure 2A, acetylated endogenous Mcm10 was readily detected by immunoblotting for acetylated lysine (K-Ac) after IP with Mcm10 antibody, demonstrating that endogenous human Mcm10 is acetylated *in vivo*. Notably, endogenous SIRT1 also co-precipitated with Mcm10 on Mcm10 IP (Figure 2A). The immunoprecipitated acetylated Mcm10 migrated as a range of subspecies close to each other, suggesting that (i) more than one domain of Mcm10 might be acetylated and/or (ii) multiple lysine residues might be acetylated in each domain (Figure 2A).

To test whether SIRT1 deacetylates Mcm10 *in vivo*, we examined the effect of SIRT1 overexpression in human cells. HCT116 cells were transiently transfected with both Mcm10- and SIRT1-expressing constructs, and complexes of these two proteins were immunoprecipitated with anti-Mcm10 antibody. As demonstrated in Figure 2B, the level of immunoprecipitated acetylated Mcm10 was decreased when SIRT1 was overexpressed. This Mcm10 deacetylation was coincident with a reduction of the total Mcm10 levels, suggesting that acetylation may regulate Mcm10 stability. Next we tested whether RNAi-mediated SIRT1 knockdown could reverse this trend. Using small double-stranded interfering RNA (siRNA) to silence SIRT1 expression (as monitored by WB analysis), we found that acetylation of Mcm10 was significantly increased by SIRT1 knockdown (Figure 2C). The reduction of the SIRT1 deacetylase activity on silencing was also evident from the higher levels of acetylated lysine residue K9 of histone H3 (H3K9), which is a well-established target of SIRT1 (Figure 2C).

Two domains of Mcm10 can be acetylated and deacetylated *in vitro*

We next examined whether Mcm10 can be acetylated *in vitro*. Purified FL Mcm10 and its NTD, ID and CTD (see Figure 1D) were incubated with recombinant p300 HAT. As shown in Figure 3A incubation of FL Mcm10 and three of its domains with p300 HAT in the presence of AcoA resulted in strong acetylation of the FL Mcm10, and of its isolated ID and CTD domains. The NT domain of Mcm10 showed no detectable acetylation by p300 HAT under similar conditions despite having a significant number of lysine residues. Furthermore, *in vitro* deacetylation assays using purified human SIRT1 in the presence of its co-factor NAD^+ or its inhibitor NIA confirmed that Mcm10 is a substrate for SIRT1 (Figure 3B and C).

We next performed mass spectrometry analysis of the *in vitro* acetylated/deacetylated Mcm10 and its domains (Table 1 and Supplementary Table S1). The analysis indicated that of four lysine residues acetylated by p300 in the ID, two residues could be specifically deacetylated by SIRT1. Furthermore, p300 acetylated nine single lysine residues and eight lysine pairs in the CTD, of which four single lysines and six pairs were specifically deacetylated by SIRT1 (Table 1 and Supplementary Table S1).

Collectively, these data show that SIRT1 modulates the acetylation status of Mcm10 via its deacetylase activity

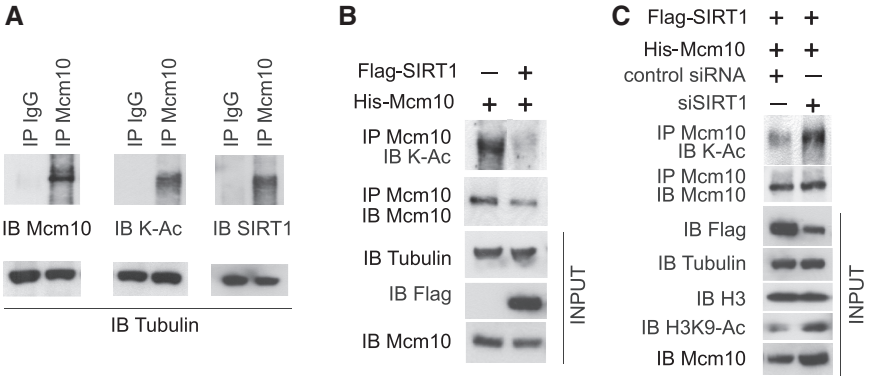

Figure 2. SIRT1 deacetylates Mcm10 *in vivo*. (**A**) Acetylated Mcm10 protein can be immunoprecipitated with anti-Mcm10 antibody from HCT116 cells. (Top panels) Left panel shows positive signal with anti-Mcm10 antibody, middle panel with anti-K-Ac antibody and right panel showing endogenous SIRT1 also co-precipitated with Mcm10. Control reactions with IgG did not immunoprecipitate Mcm10. Blots were subjected to long exposure to show all specific and non-specific protein bands. Acetylated Mcm10 migrated as a subspecies close to each other, suggesting multiple acetylation sites. (**B**) HCT116 cells were transfected with plasmids that express His-Mcm10 and Flag-SIRT1. Protein levels were determined with direct WB (input), whereas detection of Mcm10 acetylation was determined by IP of the protein with anti-Mcm10 antibody followed by WB using indicated antibodies (anti-Mcm10 and anti-K-Ac). (**C**) HCT116 cells were co-transfected with plasmids that express His-Mcm10 and Flag-SIRT1 and either siSIRT1 or control siRNA. Acetylation of Mcm10 and all protein levels were determined in a similar way to those in panel B.

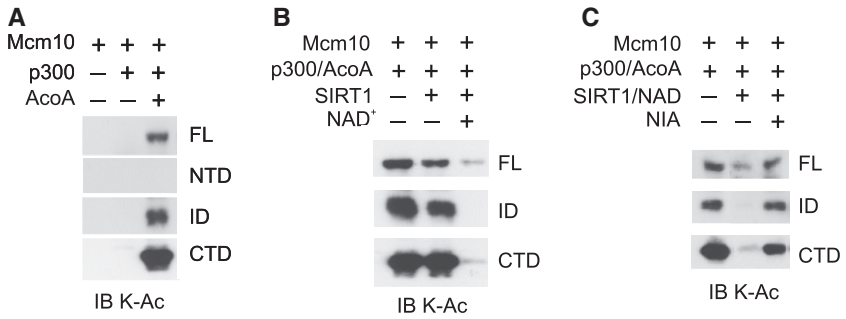

Figure 3. SIRT1 deacetylates Mcm10 *in vitro*. (**A**) Mcm10 is acetylated by p300 *in vitro*. Purified FL human Mcm10 and its three main domains (NTD, ID and CTD) were incubated for 45 min at 30°C with the recombinant p300 in the presence or absence of AcoA. Reaction products were analysed by WB with anti-K-Ac antibody as indicated. p300 can acetylate the FL Mcm10, its internal core domain and C-terminus, with the latter most efficiently acetylated. (**B**) SIRT1 deacetylates Mcm10 *in vitro* in NAD-dependent manner. The acetylation reaction products were further incubated for 45 min with the recombinant human SIRT1 in the presence or absence of NAD. (**C**) SIRT1-dependent deacetylation of Mcm10 and its domains can be inhibited by NIAThe reactions were performed in a similar way to those in (B) with addition of NIA, which specifically blocked SIRT1 activity and Mcm10 deacetylation.

targeting its two lysine-rich domains, the conserved ID and the metazoan-specific CTD. Acetylation and deacetylation of Mcm10 modulate its DNA binding. Because the ID and CTD of Mcm10 can both be acetylated by p300 and deacetylated by SIRT1 *in vitro* (Figure 3) and are known DNA-interacting domains, we examined the effect of acetylation and deacetylation on the DNA-binding properties of these domains. Electrophoretic mobility assays (EMSA) with a 60-nt long ssDNA probe were used for these experiments. Figure 4 shows that the purified recombinant CTD efficiently binds ssDNA (lanes 2 and 3). This DNA binding, however, was reduced (~2.5-fold) on acetylation by p300 (Figure 4A, compare lanes 2 and 3 with 4 and 5, and Supplementary Figure S1A, bars 2 and 3). On the other hand, addition of SIRT1 to deacetylate the CTD restored DNA binding (Figure 4A, lanes 6 and 7, and Supplementary Figure S1A, bars 3 and 4). A small increase in CTD DNA binding was observed when SIRT1 was present in the reaction with NAD^+ (~10%, Figure 4A, lanes 8 and 9, and Supplementary Figure S1A, bars 2 and 5). No significant change of DNA-binding efficiency of CTD was observed in the presence of substrateless SIRT1 (Supplementary Figure S2).

A different set of results was obtained when the ID of Mcm10 was tested under identical conditions. The interaction of this domain with DNA was minimal when the non-modified ID was used, but greatly enhanced on addition of p300 to the reaction mix (~3.5-fold, Figure 4B, lanes 2 and 3 compared with lanes 4 and 5, and Supplementary Figure S1B, bars 2 and 3). Interestingly, this increased DNA-binding ability was not affected by the subsequent deacetylation by SIRT1 (Figure 4B, lanes 6 and 7, and Supplementary Figure S1B, bars 3 and 4). Furthermore, the presence of SIRT1 increased DNA binding of ID ~2-fold (Figure 4B, lanes 8 and 9, and Supplementary Figure S1B, lanes 2 and 5). Finally, when the FL Mcm10 was tested, addition of p300 to the reaction mix increased its DNA-binding property (~6.5-fold, Figure 4C, compare lanes 2 and 3 with lanes 4 and 5, and Supplementary Figure S1C, bars 2 and 3). Moreover, the DNA binding of Mcm10 was

Table 1. Mcm10 lysine residues acetylated by p300 and deacetylated by SIRT1 *in vitro*, as determined by mass spectrometry of the recombinant Mcm10 domains

Mcm10 domain	Lysine (K) residues acetylated by p300	Lysine (K) residues still acetylated after SIRT1 treatment	Lysine (K) residues deacetylated by SIRT1
ID	K267	K267	
	K312		**K312**
	K318	K318	
	K390		**K390**
CTD	K657	K657	
	K664	K664	
	K681	K681	
	K683		**K683**
	K745		**K745**
	K761		**K761**
	K768		**K768**
	K783	K783	
	K853	K853	
CTD (double sites)	**K681 + K682**		**K681 + K682**
	K737 + K739		**K737 + K739**
	K847 + K849		**K847 + K849**
	K868 + K874		**K868 + K874**
	K683 + K685		**K683 + K685**
	K674 + K682		**K674 + K682**
	K674 + K681	K674 + K681	
	K668 + K674	K668 + K674	

Acetylated lysine residues that are targets for SIRT1 deacetylation are in bold. Supplementary Table S1 contains additional information regarding protein probability scores, sequence coverage and peptide sequences for each Mcm10 product.

further enhanced by SIRT1-mediated deacetylation (~1.5-fold, Figure 4C, lanes 6 and 7, and Supplementary Figure S1C, bars 3 and 4). The FL Mcm10 protein DNA binding was not affected by the addition of SIRT1 (with NAD+), which has slightly enhanced the DNA binding of Mcm10 ID (Figure 4B and C, lanes 8 and 9). Presumably some epitopes of the ID may be less accessible for SIRT1 interaction within hexameric assembly of Mcm10 and/or this interaction may be less efficient and provide less effect at the gel-shift conditions.

In parallel with the EMSA experiments, we examined whether acetylation and/or deacetylation of the Mcm10 domains took place under conditions used for the EMSA experiments. Aliquots of the samples loaded onto EMSA gels were resolved on 4–12% PAAG gels and immunoblotted with anti-K-Ac antibody (Figure 4D, lanes 1, 3, 4 and 5). The analysis showed that the presence of ssDNA did not interfere with p300-mediated acetylation of the CTD, and the domain was acetylated by p300 regardless of whether the DNA or p300 was added first to CTD (Figure 4D, top panel). These results suggest that either the acetyltransferase can compete for lysine residues on the Mcm10 CTD when it is bound to DNA, or that not all lysine residues targeted by p300 are involved in DNA binding. Furthermore, when SIRT1 was added to the reactions, it could deacetylate CTD lysines in the absence or presence of DNA, and also when DNA was added to the solution before or after SIRT1. These results indicated that samples resolved on lanes 4 and 5 of the EMSA experiment (Figure 4A) contained acetylated CTD, and the CTD resolved on lanes 6 and 7 was deacetylated (Figure 4A).

On the contrary, the ID pre-incubated with ssDNA was not accessible for acetylation (Figure 4D, lane 2, bottom panel). The ID was acetylated less efficiently when p300 HAT was given a "head-start" before the addition of ssDNA (Figure 4D, lane 3, bottom panel). The subsequent addition of SIRT1 could efficiently deacetylate the ID regardless of the presence of DNA.

SIRT1 depletion affects Mcm10 levels on and off chromatin

Having demonstrated a SIRT1-dependent effect on Mcm10 binding to DNA *in vitro*, we tested the effect of SIRT1 knockdown on Mcm10 binding to chromatin *in vivo*. To that end, HCT116 cells were first synchronized by thymidine block for 24 h, followed by RNAi (transfection with siSIRT1 or control siRNA) for another 24 h, after which the medium was replaced with thymidine-only-containing medium, and cells were incubated further for 12 h until their release into S-phase and sample collection during the next 8 h (Figure 5A).

We first analysed the levels of the nuclear soluble Mcm10 (Figure 5B). At time point zero, just before the release into the S-phase, the levels of Mcm10 were higher when SIRT1 was depleted, and these higher levels persisted throughout the time course, whereas Mcm2 appeared unchanged (Figure 5B). These results are consistent with those shown in Figure 2C showing that SIRT1 depletion resulted in slight increase of total Mcm10 in asynchronous cell culture. Notably, the time points that spanned S-phase and the beginning of G2/M phase showed an extra band (Mcm10*) reactive with anti-Mcm10 antibody and running just under the main band

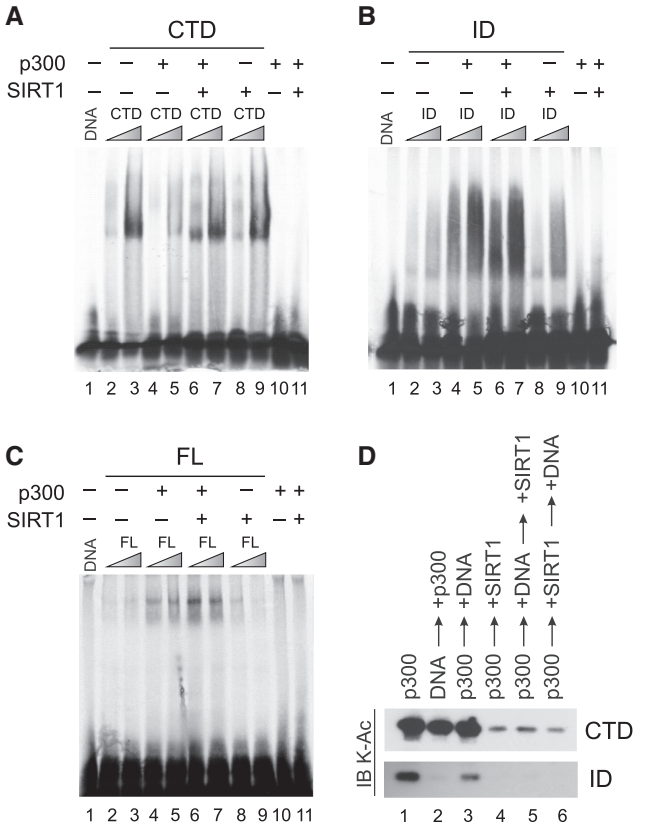

Figure 4. Acetylation and deacetylation modulate properties of Mcm10 DNA-binding domains in a distinct way. ^{33}[P]-labelled ssDNA of 60 nt length was used for EMSA analysis. Purified Mcm10 or its domains were first incubated in the presence or absence of p300 and AcoA, and/or SIRT1 and NAD under conditions identical to those shown in Figure 3. Reaction mix containing either acetylated or deacetylated Mcm10 (or its domain) was then incubated with ssDNA and protein–DNA complexes formed were analysed on 6% Polyacrylamide gel (PAAG). (**A**) Acetylation negates DNA binding of CTD. Untreated CTD efficiently formed complexes with DNA (lanes 2 and 3), whereas acetylated CTD did not (lanes 4 and 5). Deacetylation by SIRT1 restored DNA binding by CTD (lanes 6 and 7). Addition of SIRT1 (and NAD^+) to CTD did not substantially enhance its DNA binding (lanes 8 and 9). Neither p300 nor SIRT1 formed complexes with ssDNA on their own (lanes 10 and 11, respectively). (**B**) Acetylation of the ID of Mcm10 enhanced its DNA binding (lanes 4 and 5 compared with 2 and 3). Subsequent deacetylation with SIRT1 did not negate it (lanes 6 and 7). (**C**) Acetylation of the FL Mcm10 stimulated DNA-complex formation (lanes 2 and 3), which was further enhanced by subsequent deacetylation with SIRT1 (lanes 6 and 7). Lane 1 on all gels—DNA probe without any protein. (**D**) DNA interferes with acetylation of ID but not CTD of Mcm10. DNA was added to Mcm10 domains before or after addition of p300/AcoA or SIRT1/NAD^+. Products of reactions were analysed by WB with anti-K-Ac antibody, similar to Figure 3. Lanes 3 and 6 represent reactions identical to those used for EMSA. The presence of DNA inhibited acetylation of ID when added before p300 (lane 2).

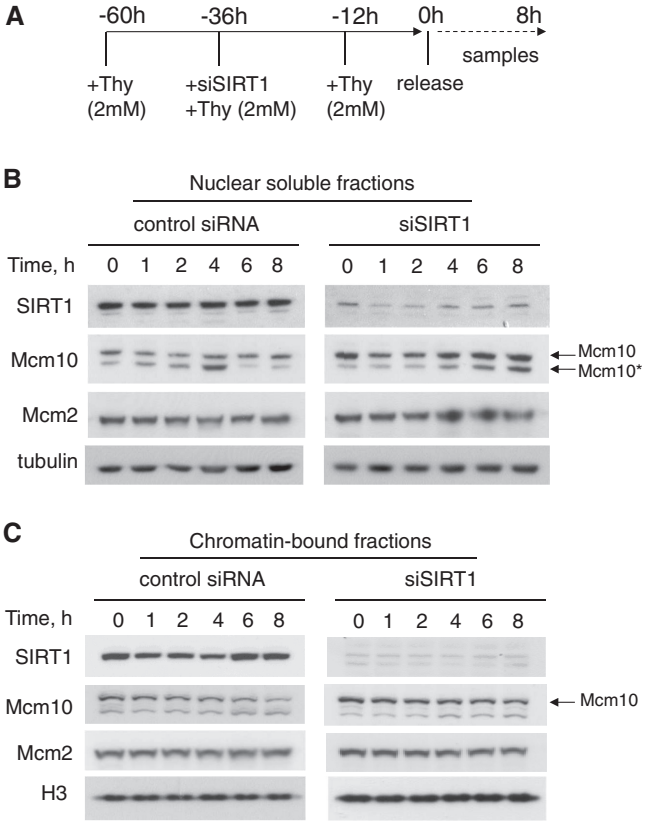

Figure 5. Depletion of SIRT1 modulates Mcm10 levels on and off chromatin. HCT116 cells were synchronized by the thymidine block, treated with anti-SIRT1 and control siRNAs in the presence of thymidine, and released into S-phase with samples collected during the next 8 h (**A**). Cell extracts were fractionated to analyse nuclear soluble and chromatin-bound proteins (**B** and **C**). The levels of nuclear soluble Mcm10 were higher when SIRT1 was depleted compared with respective samples obtained from cells treated with control siRNA, whereas levels of Mcm2 and tubulin were unchanged (right versus left panels, B). Notably, the levels of a post-translationally modified form of Mcm10 (Mcm10*) that migrated below Mcm10 accumulated during the S-phase were lower when control cells entered G2/M (time points 6 and 8 h, left panel, B). However, this Mcm10* specie did not disappear during G2/M in cells with depleted SIRT1 (right panel, B). The analysis of chromatin-bound Mcm10 shows that higher levels of Mcm10 are associated with chromatin from the beginning to the end of the time course in cells with depleted SIRT1, whereas Mcm2 levels and histone 3 (H3) remained unchanged (C).

of Mcm10 (Figure 4B). This Mcm10* specie was especially prominent at the end of the S-phase but disappeared when cells treated with the control siRNA entered G2/M, suggesting that it might correspond to a differently post-translationally modified Mcm10, e.g. Mcm10 with low phosphorylation status, which is known to accumulate at the end of S-phase and is subsequently being destroyed during G2 (8,13). This was not the case, however, for cells with depleted SIRT1. The Mcm10* species slowly accumulated throughout the time course and did not disappear, suggesting that the absence of SIRT1 might change Mcm10 post-translational modification dynamics and turnover (Figure 4B).

The analysis of chromatin-bound Mcm10 showed that again, in cells with depleted SIRT1, higher levels of Mcm10 were associated with chromatin from the beginning to the end of the time course, whereas Mcm2 levels remained unchanged (Figure 4C). Only a small and relatively unchanged amount of Mcm10* (or similar) species was present on chromatin.

SIRT1 and Mcm10 depletion affect cell cycle and DNA replication

Having demonstrated a specific interaction between Mcm10 and SIRT1 and SIRT1-dependent modulation of

Mcm10 binding to DNA, we next analysed the effects of Mcm10 and/or SIRT1 knockdown on overall DNA synthesis and cell cycle. For this purpose, we performed RNAi-mediated knockdown of Mcm10 and SIRT1 individually and together. DNA synthesis and total DNA were analysed 48 h after siRNA transfection (Figure 6). Mcm10 knockdown produced a significant decrease (>2-fold) in the number of S-phase cells (Figure 6B and E). This was accompanied by an increase in G1-phase cell population and a small decrease in G2/M-phase cell population (Figure 6B). These results suggest that Mcm10 knockdown diminishes overall DNA synthesis (BrdU uptake), which is consistent with Mcm10 role as an essential DNA replication initiation factor. SIRT1 knockdown also produced a significant change in cell cycle profile (Figure 6C) with a substantial (~2-fold) increase in the G2/M-phase cell population, while the S-phase cell population remained relatively unchanged (Figure 6C and E). Simultaneous knockdown of both Mcm10 and SIRT1 resulted in ~2-fold reduction in the number of S-phase cells and an increase of the G1 population, which was similar to the effects of knocking down Mcm10 alone (Figure 6D and E). In addition, Mcm10 depletion, either alone or in combination with SIRT1 knockdown resulted in a pronounced reduction in overall DNA synthesis (BrdU uptake) (Figure 6B, D and E). Longer (72 h) post-transfection incubation resulted in significant cell death for both Mcm10 and SIRT1 depletions (not shown).

To test the possibility that Mcm10 and/or SIRT1 depletion resulted in DNA damage, we monitored the phosphorylated form of histone H2AX (γH2AX) (56). Accumulation of γH2AX was evident in all three cases and was at highest level when both Mcm10 and SIRT1 were simultaneously depleted (Figure 6F), indicating the induction of DNA damage on SIRT1 and Mcm10 depletion.

SIRT1 and Mcm10 depletion affects origin activation and replication fork velocity

To investigate the effect of Mcm10 and/or SIRT1 depletion on DNA replication, we used a single DNA molecule approach based on DNA combing (51,57,58). Human Mcm10 and SIRT1 were silenced in HCT116 cells by siRNAs individually and simultaneously, as described above. Representative images of replication signals are shown in Figure 7A for cells treated with control siRNA (top) and for cells simultaneously knocked down for SIRT1 and Mcm10 (bottom). Distances between replication origins and fork velocities were calculated and the analysis is reported in Figure 7B and C, respectively.

The inter-origin distances decreased slightly when Mcm10 was knocked down. Thus, >60% of the inter-origin distances in this sample were lower than the mean value of the control (Figure 7B). SIRT1 depletion did not change the value of inter-origin distances. When both proteins were knocked down simultaneously, we observed a strong reduction of inter-origin distances, with the mean value reduced from 120 kb to 92 kb ($P < 0.001$) (Figure 7B).

The average velocity of replication forks remained relatively unchanged when Mcm10 was knocked down, and went slightly up to 1.53 kb/min ($P < 0.01$) in cells transfected with siRNA targeting SIRT1, showing that forks tend to accelerate when SIRT1 protein levels are reduced (Figure 7C). In contrast, when both SIRT1 and Mcm10 were depleted at the same time, fork velocity went significantly downward from 1.35 to ~1 kb/min ($P < 0.001$), indicating that simultaneous knockdown of Mcm10 and SIRT1 slows down replication fork progression (Figure 7C, bottom panel). The reduction in fork velocity and inter-origin distance in cells with simultaneous knockdown of Mcm10 and SIRT1 coincided with higher level of DNA damage as monitored by induction of γH2AX (Figure 6F).

DISCUSSION

Our study shows that human Mcm10 is an acetylated protein regulated by SIRT1, which specifically binds and deacetylates Mcm10 both *in vivo* and *in vitro*. The interaction between Mcm10 and SIRT1 can be mapped to the CTD of Mcm10; however, it does not require C-terminal Zn-finger motifs and does not interfere with DNA binding (Figure 1). Importantly, both DNA-binding domains of Mcm10, ID and CTD can be acetylated by p300 HAT, with the CTD being the more efficient recipient of the modification at least *in vitro* (Figure 3 and Table 1). The prediction of lysine acetylation sites in Mcm10 by the PAIL software suggests there are multiple possible targets in both lysine-rich ID and CTD parts of Mcm10 protein (59,60). This was further confirmed by the mass spectrometry analysis of recombinant Mcm10 domains acetylated by p300 (Table 1).

The subsequent SIRT1-catalysed deacetylation of either domain can be blocked by the addition of NIA, an inhibitor of sirtuins, thus confirming the specific nature of the reaction (Figure 3). Similarly, SIRT1-dependent deacetylation *in vivo* can be diminished by depleting SIRT1 levels with siRNA (Figure 2). Moreover, SIRT1 specifically deacetylated a set of lysine residues within ID and CTD Mcm10 domains when tested *in vitro* (Table 1).

We also analysed the effect of acetylation and deacetylation of Mcm10 (and its domains) on DNA binding. Interestingly, the experiments showed that the two DNA-binding domains of Mcm10 are modulated in distinct fashion. Acetylation of the Mcm10 ID stimulates DNA binding, whereas acetylation of the CTD inhibits DNA binding. However, the latter can be restored by SIRT1-dependent deacetylation of CTD (Figure 4).

Chromatin recruitment of Mcm10 was also affected when SIRT1 was depleted by siRNA during S-phase, that is, more Mcm10 was loaded and retained on chromatin throughout the S-phase consistently with the overall higher levels of Mcm10 on SIRT1 silencing (Figure 5).

Additionally, we also investigated the global effect of Mcm10 and SIRT1 depletion by siRNA on the cell cycle and DNA replication. Depletion of Mcm10 led to an aberrant S-phase and drastic decrease of

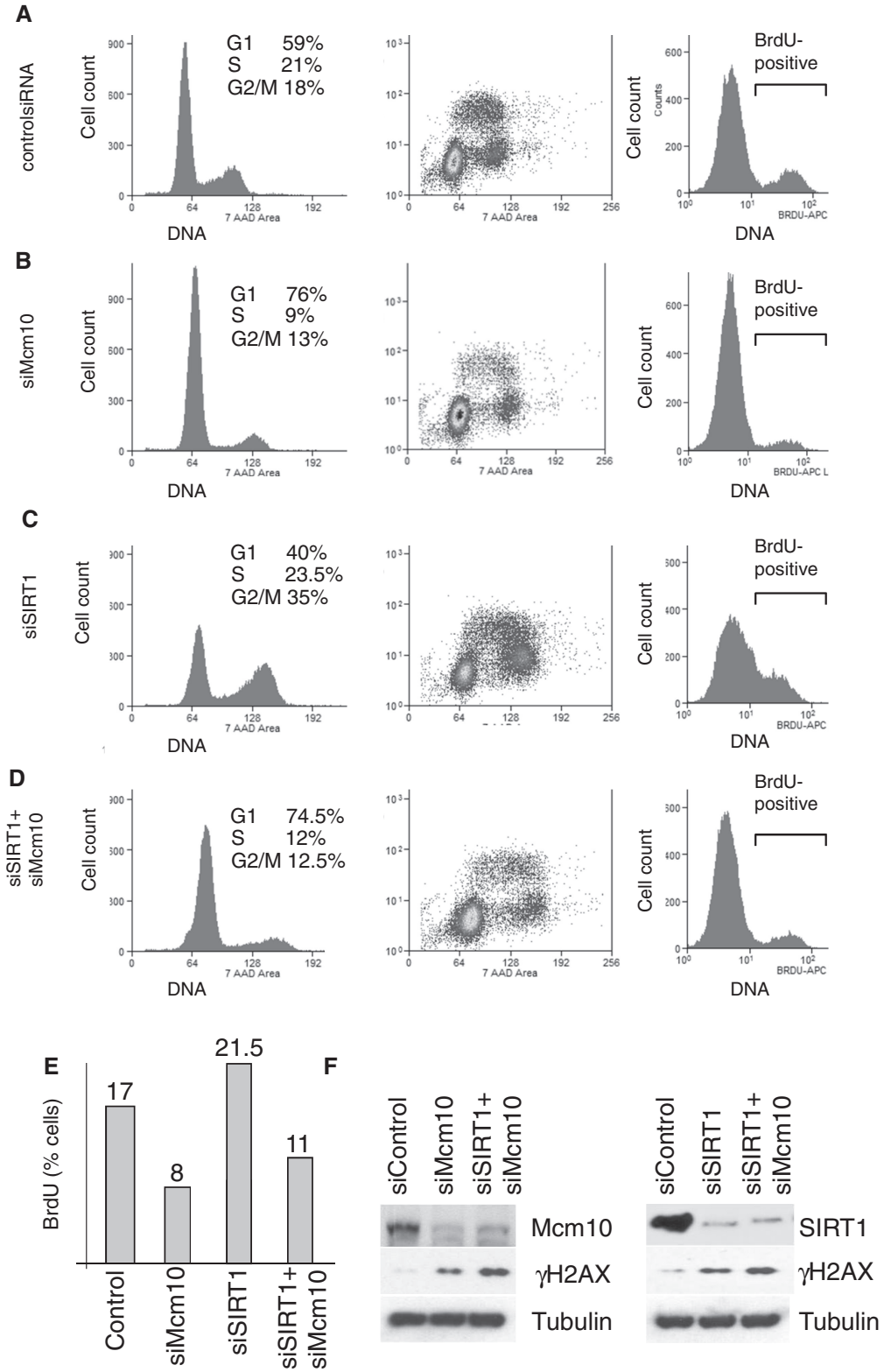

Figure 6. Depletion of SIRT1 affects DNA replication. FACS analysis of HCT116 cells after depletion of Mcm10 and/or SIRT1 levels with siRNAs. Cell cycle profile and BrdU incorporation of HCT116 cells 48 h after being transfected with (**A**) control siRNA, (**B**) siMcm10, (**C**) siSIRT1, (**D**) both Mcm10 and SIRT1 siRNAs. (**E**) Comparison of BrdU incorporation levels (active DNA synthesis) in HCT116 cells after Mcm10 and/or SIRT1 depletion. (**F**) Induction of γH2AX in cells with downregulated Mcm10 and/or SIRT1.

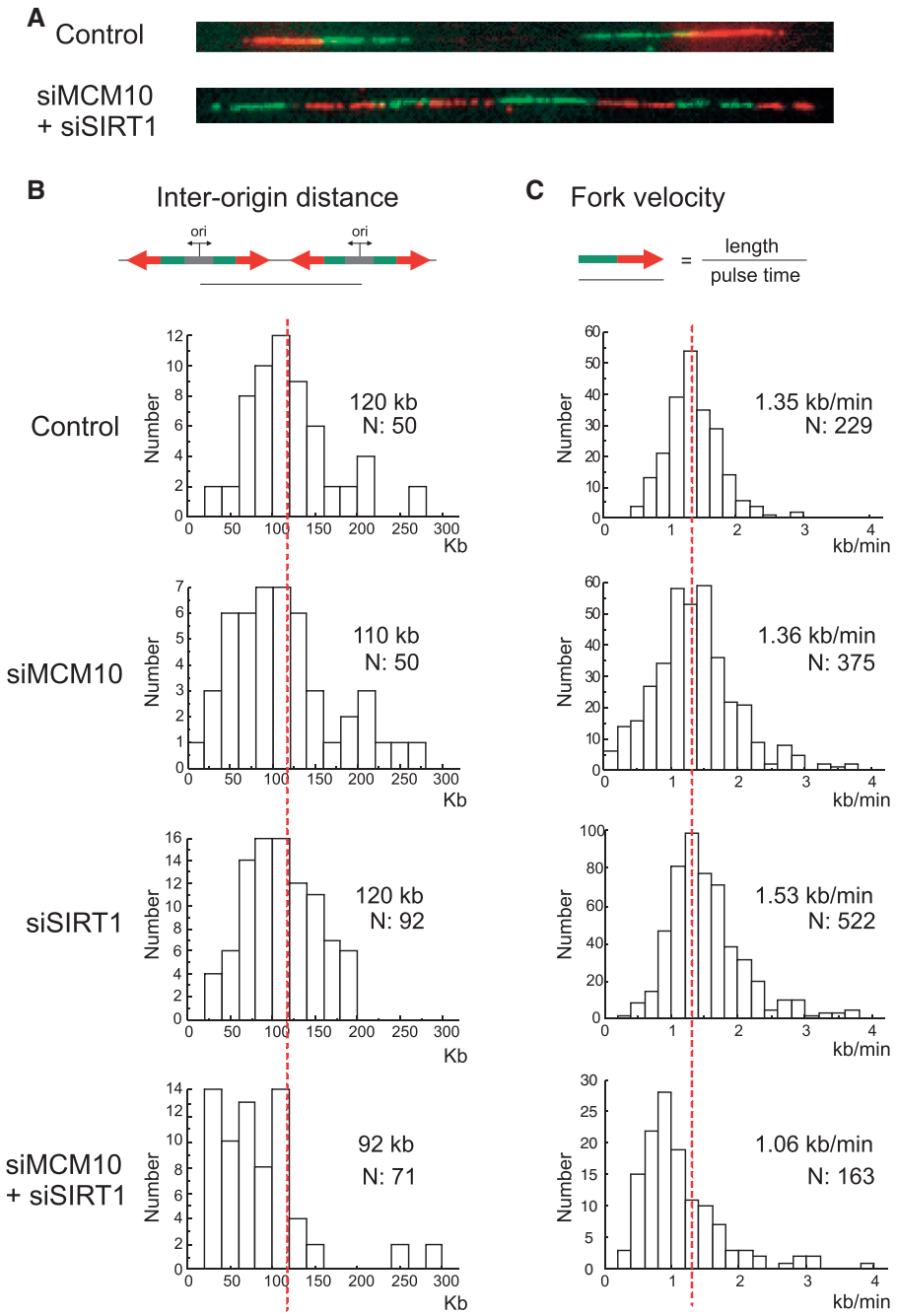

Figure 7. Depletion of Mcm10 and SIRT1 affects origin activation and replication fork velocity. (**A**) Representative images of combed DNA fibres. (**B**) Inter-origin distances were measured on individual DNA molecules from HCT116 cells transfected with indicated siRNAs. (**C**) Fork velocity was measured as the average of contiguous IdU- and CldU-labelled tracks divided by their pulse time (20 min each). Mean values are indicated, respectively, for fork velocity and for inter-origin plots. Red dashed lines indicate median values for control HCT116 cells transfected with control siRNA.

BrdU-incorporating S-phase population, whereas SIRT1-depleted cells showed slight increase in S-phase cell population and significant accumulation in G2/M phase. DNA damage signalling resulting from Mcm10 and/or SIRT1 depletion suggested that replication forks were not efficiently stabilized and/or repaired when DNA replication was initiated under those conditions (Figure 6). Furthemore, when both SIRT1 and Mcm10 were depleted, cells experienced problems with both initiation and progression of DNA synthesis (Figures 6 and 7), suggesting that Mcm10–SIRT1 partnership may function in both the initiation and the elongation phases of DNA replication.

SIRT1 role in Mcm10 regulation

Previous studies in yeast have demonstrated that yeast Mcm10 can interact with Sir2 and act as a bridge to link Sir2 to other components of the DNA replication machinery; however, it has not been shown whether Mcm10 is a

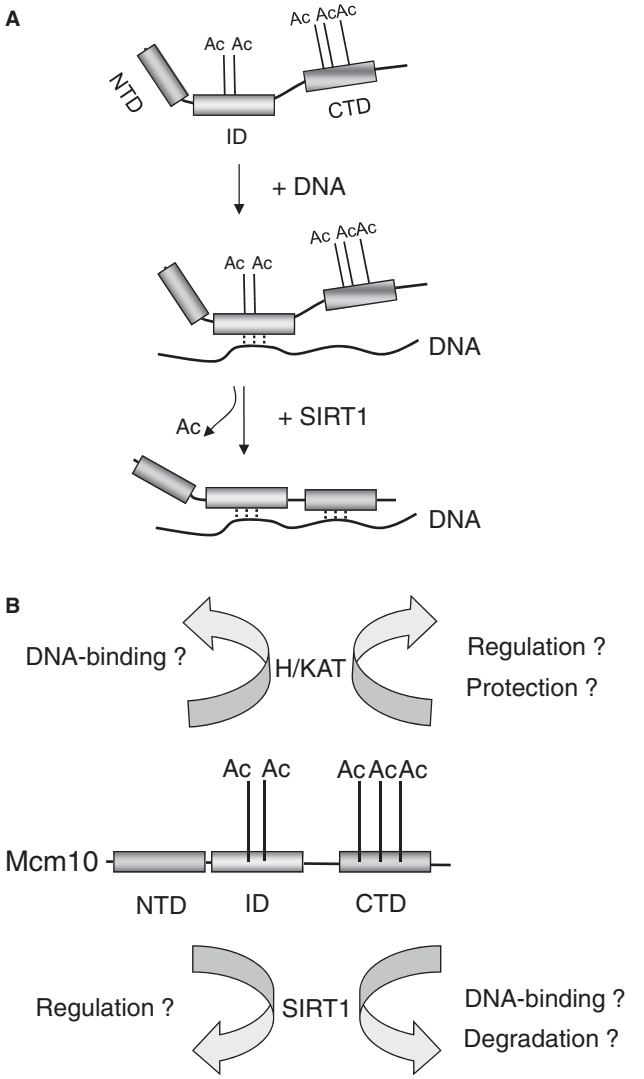

Figure 8. Schematic model of the Mcm10 regulation by acetylation and SIRT1. (**A**) Acetylation of Mcm10 promotes DNA binding of the conserved ID, but negates DNA binding of the metazoan-specific CTD. The acetylation of ID serves for the initial Mcm10 loading onto DNA via its OB-fold domain, with further deacetylation of CTD needed to stabilize the complex and provide additional Mcm10-DNA and Mcm10-protein contacts. (**B**) Deacetylation of Mcm10 at CTD could also deprotect it from ubiquitination.

subject of Sir2-dependent deacetylation (40–42). Our data now indicate that the Sir2 human ortholog, SIRT1, plays a direct regulatory role in DNA replication in human cells by modifying Mcm10.

Collectively, our data suggest a model of acetylation/deacetylation-dependent regulation of Mcm10 DNA binding (Figure 8A). Acetylation could be required for the initial DNA binding via the conserved ID (in keeping with the data in Figure 4B), possibly at the stage of the replisome assembly. It is also possible that the acetylation of some lysine residues in the ID sequence may serve as a temporary block that directs this domain (and Mcm10) into a certain type of interaction with DNA and/or proteins and then can be removed to allow a next step interaction during multiprotein replisome complex assembly. For example, the acetylation of lysine residues in the ID may promote the binding of Mcm10 to DNA via its OB (oligonucleotide/oligosaccharide binding)-fold domain using hydrophobic interactions. Subsequent deacetylation of the ID bound to DNA would not affect the DNA complex stability and may unprotect lysine residues that can then either serve to provide an additional interaction with DNA or participate in protein–protein interaction within the DNA replication complex. The following SIRT1-dependent deacetylation of the CTD may then fully potentiate the DNA-binding capacity of Mcm10.

In addition to the DNA-binding modulation of Mcm10 by SIRT1, our data suggest that deacetylation may also unprotect lysine residues that are otherwise ubiquitinated marking Mcm10 for degradation (Figure 8B). Consistent with this, the overexpression of SIRT1 led to decrease of Mcm10 levels (Figure 2). This observation is also consistent with a recently published report that the C-terminal part of Mcm10 is required for its degradation (61,62). Furthermore, the depletion of SIRT1 led to stabilization of the Mcm10 levels overall and especially during mitosis (Figure 5), indicating that SIRT1 plays an important role in regulating Mcm10 degradation.

SIRT1 role in regulation of DNA replication

There are a number of recent reports on the importance of protein acetylation in regulation of DNA replication. Thus, in yeast, acetylation of multiple lysine residues on histone H3 and H4 tails facilitates origin firing (28). However, local histone acetylation does not reflect origin efficiencies in mammalian fibroblasts, at least in euchromatic transcribed regions (63). Nevertheless, DNA replication origin licensing by Cdt1 and Mcm2–7 loading in human cells is mediated by HBO1, Orc1 interacting acetyltransferase, which acetylates histone H4 (64–66). Furthermore, recent reports showed that cohesin acetylation facilitates replication fork processivity, deacetylation of Cdt1 by HDAC11 regulates its stability, acetylation of Cdc6 modulates its phosphorylation and acetylation of DNA2 and FEN1 regulates their nuclease activity (67–70).

Previous studies in yeast have demonstrated Sir2-dependent negative regulation of a subset of DNA replication origins (36,38). These studies suggested an involvement of Sir2, at least indirectly via remodelling chromatin, in early steps of preRC assembly most likely through its deacetylase activity. Our results show that, on its own, SIRT1 depletion increases replication fork velocity, but a simultaneous depletion of SIRT1 and Mcm10 significantly reduces replication fork velocity and inter-origin distance.

DNA molecular combing and cell cycle analyses demonstrate that the depletion of Mcm10 deregulates origin activation and leads to DNA damage signalling and reduction of cell numbers in S-phase (Figures 6 and 7, respectively). Depletion of SIRT1 on the other hand leads to DNA damage and higher fork velocity (Figures 6F and 7B). This acceleration may result from chromatin being more relaxed due to the lack of SIRT1, and thus,

forks encounter less hindrance during progression. Additionally the depletion of SIRT1 might directly or indirectly affect acetylation/deacetylation balance of cohesins, thus again, facilitating fork progression. It is also possible that lack of SIRT1 activity shifts the balance in timing of origin firing similar to what has been observed in yeast rendering late origins to fire earlier (36–39).

The simultaneous depletion of Mcm10 and SIRT1 appears to act in a synergistic manner and results in significant slowing down of forks, higher DNA-damage signalling and drastic reduction of inter-origin distances (Figure 7), resulting most likely from the activation of dormant origins within the same replisome clusters (51,71–74). A possible reason for such synergistic effect of the simultaneous Mcm10/SIRT1 knockdown is that the individual knockdowns were not complete and left enough of respective protein targets to initiate DNA replication origins. The amount of deacetylated Mcm10 was, however, severely decreased when both Mcm10 and SIRT1 were depleted. Taken together, this suggests that deacetylation of Mcm10 by SIRT1 is one of the important regulatory events in initiation of forks and that the acetylation/deacetylation balance of Mcm10 has to be regulated tightly for both proper fork initiation and progression. One can envisage that distinct patterns of acetylation/deacetylation of Mcm10 might be required for the different steps of DNA replication.

When this manuscript was in preparation, three reports were published showing that Mcm10 has a new important role in DNA replication initiation (75–77). Thus, Mcm10 facilitates the Mcm2–7 promoted origin DNA unwinding step (75–77). Future experiments will help to establish whether the SIRT1-dependent deacetylation regulates this role of Mcm10.

Overall, our findings demonstrate SIRT1-dependent regulation of an essential DNA replication factor Mcm10 and highlight the importance of protein acetylation for DNA replication. Furthermore, our data provide a first link between DNA replication and sirtuin deacetylases, suggesting a possible crosstalk between cellular circuits of the cell cycle, metabolism and DNA synthesis.

SUPPLEMENTARY DATA

Supplementary Data are available at NAR Online: Supplementary Table 1, Supplementary Figures 1 and 2 and Supplementary Methods.

ACKNOWLEDGEMENTS

The authors would like to thank Prof. Fuyuki Ishikawa and Dr Nobuyuki Tanimura (Kyoto University, Japan) for the kind gift of pCDNA3.1-Flag-hSIRT1 construct and pGEX-5X-hSIRT1; Dr Eric Verdin for provision of expression constructs for Flag-SIRT2, -5, -6 and -7; Dr Warner Greene for provision of expression construct for p300. The authors are grateful to Prof. Jo Milner (University of York, UK) for helpful comments and discussions.

FUNDING

MRC New Investigator Research [G0700001 to A.O.]; Intramural Program of the US National Cancer Institute, Center for Cancer Research [Z01 BC 006150-19LMP to Y.P.]; Wellcome Trust Grant (to J.G.Z.). Funding for open access charge: MRC.

Conflict of interest statement. None declared.

REFERENCES

1. Bell,S.P. and Dutta,A. (2002) DNA replication in eukaryotic cells. *Annu. Rev. Biochem.*, **71**, 333–374.
2. Costa,S. and Blow,J.J. (2007) The elusive determinants of replication origins. *EMBO Rep.*, **8**, 332–334.
3. Mendez,J. and Stillman,B. (2003) Perpetuating the double helix: molecular machines at eukaryotic DNA replication origins. *Bioessays*, **25**, 1158–1167.
4. Remus,D. and Diffley,J.F. (2009) Eukaryotic DNA replication control: lock and load, then fire. *Curr. Opin. Cell Biol.*, **21**, 771–777.
5. Gregan,J., Lindner,K., Brimage,L., Franklin,R., Namdar,M., Hart,E.A., Aves,S.J. and Kearsey,S.E. (2003) Fission yeast Cdc23/Mcm10 functions after pre-replicative complex formation to promote Cdc45 chromatin binding. *Mol. Biol. Cell*, **14**, 3876–3887.
6. Homesley,L., Lei,M., Kawasaki,Y., Sawyer,S., Christensen,T. and Tye,B.K. (2000) Mcm10 and the MCM2-7 complex interact to initiate DNA synthesis and to release replication factors from origins. *Genes Dev.*, **14**, 913–926.
7. Izumi,M., Yanagi,K., Mizuno,T., Yokoi,M., Kawasaki,Y., Moon,K.Y., Hurwitz,J., Yatagai,F. and Hanaoka,F. (2000) The human homolog of *Saccharomyces cerevisiae* Mcm10 interacts with replication factors and dissociates from nuclease-resistant nuclear structures in G(2) phase. *Nucleic Acids Res.*, **28**, 4769–4777.
8. Izumi,M., Yatagai,F. and Hanaoka,F. (2001) Cell cycle-dependent proteolysis and phosphorylation of human Mcm10. *J. Biol. Chem.*, **276**, 48526–48531.
9. Lee,J.K., Seo,Y.S. and Hurwitz,J. (2003) The Cdc23 (Mcm10) protein is required for the phosphorylation of minichromosome maintenance complex by the Dfp1-Hsk1 kinase. *Proc. Natl Acad. Sci. USA*, **100**, 2334–2339.
10. Okorokov,A.L., Waugh,A., Hodgkinson,J., Murthy,A., Hong,H.K., Leo,E., Sherman,M.B., Stoeber,K., Orlova,E.V. and Williams,G.H. (2007) Hexameric ring structure of human MCM10 DNA replication factor. *EMBO Rep.*, **8**, 925–930.
11. Sawyer,S.L., Cheng,I.H., Chai,W. and Tye,B.K. (2004) Mcm10 and Cdc45 cooperate in origin activation in *Saccharomyces cerevisiae*. *J. Mol. Biol.*, **340**, 195–202.
12. Wohlschlegel,J.A., Dhar,S.K., Prokhorova,T.A., Dutta,A. and Walter,J.C. (2002) Xenopus Mcm10 binds to origins of DNA replication after Mcm2-7 and stimulates origin binding of Cdc45. *Mol. Cell*, **9**, 233–240.
13. Izumi,M., Yatagai,F. and Hanaoka,F. (2004) Localization of human Mcm10 is spatially and temporally regulated during the S phase. *J. Biol. Chem.*, **279**, 32569–32577.
14. Fien,K. and Hurwitz,J. (2006) Fission yeast Mcm10p contains primase activity. *J. Biol. Chem.*, **281**, 22248–22260.
15. Fien,K., Cho,Y.S., Lee,J.K., Raychaudhuri,S., Tappin,I. and Hurwitz,J. (2004) Primer utilization by DNA polymerase alpha-primase is influenced by its interaction with Mcm10p. *J. Biol. Chem.*, **279**, 16144–16153.
16. Ricke,R.M. and Bielinsky,A.K. (2004) Mcm10 regulates the stability and chromatin association of DNA polymerase-alpha. *Mol. Cell*, **16**, 173–185.

17. Zhu,W., Ukomadu,C., Jha,S., Senga,T., Dhar,S.K., Wohlschlegel,J.A., Nutt,L.K., Kornbluth,S. and Dutta,A. (2007) Mcm10 and And-1/CTF4 recruit DNA polymerase alpha to chromatin for initiation of DNA replication. *Genes Dev.*, **21**, 2288–2299.
18. Warren,E.M., Huang,H., Fanning,E., Chazin,W.J. and Eichman,B.F. (2009) Physical interactions between Mcm10, DNA, and DNA polymerase alpha. *J. Biol. Chem.*, **284**, 24662–24672.
19. Robertson,P.D., Chagot,B., Chazin,W.J. and Eichman,B.F. (2010) Solution NMR structure of the C-terminal DNA binding domain of Mcm10 reveals a conserved MCM motif. *J. Biol. Chem.*, **285**, 22942–22949.
20. Robertson,P.D., Warren,E.M., Zhang,H., Friedman,D.B., Lary,J.W., Cole,J.L., Tutter,A.V., Walter,J.C., Fanning,E. and Eichman,B.F. (2008) Domain architecture and biochemical characterization of vertebrate Mcm10. *J. Biol. Chem.*, **283**, 3338–3348.
21. Warren,E.M., Vaithiyalingam,S., Haworth,J., Greer,B., Bielinsky,A.K., Chazin,W.J. and Eichman,B.F. (2008) Structural basis for DNA binding by replication initiator Mcm10. *Structure*, **16**, 1892–1901.
22. Pacek,M., Tutter,A.V., Kubota,Y., Takisawa,H. and Walter,J.C. (2006) Localization of MCM2-7, Cdc45, and GINS to the site of DNA unwinding during eukaryotic DNA replication. *Mol. Cell*, **21**, 581–587.
23. Park,J.H., Bang,S.W., Jeon,Y., Kang,S. and Hwang,D.S. (2008) Knockdown of human MCM10 exhibits delayed and incomplete chromosome replication. *Biochem. Biophys. Res. Commun.*, **365**, 575–582.
24. Park,J.H., Bang,S.W., Kim,S.H. and Hwang,D.S. (2008) Knockdown of human MCM10 activates G2 checkpoint pathway. *Biochem. Biophys. Res. Commun.*, **365**, 490–495.
25. Das-Bradoo,S., Ricke,R.M. and Bielinsky,A.K. (2006) Interaction between PCNA and diubiquitinated Mcm10 is essential for cell growth in budding yeast. *Mol. Cell. Biol.*, **26**, 4806–4817.
26. Choudhary,C., Kumar,C., Gnad,F., Nielsen,M.L., Rehman,M., Walther,T.C., Olsen,J.V. and Mann,M. (2009) Lysine acetylation targets protein complexes and co-regulates major cellular functions. *Science*, **325**, 834–840.
27. Hu,L.I., Lima,B.P. and Wolfe,A.J. (2010) Bacterial protein acetylation: the dawning of a new age. *Mol. Microbiol.*, **77**, 15–21.
28. Unnikrishnan,A., Gafken,P.R. and Tsukiyama,T. (2010) Dynamic changes in histone acetylation regulate origins of DNA replication. *Nat. Struct. Mol. Biol.*, **17**, 430–437.
29. Yang,X.J. and Seto,E. (2008) Lysine acetylation: codified crosstalk with other posttranslational modifications. *Mol. Cell*, **31**, 449–461.
30. Blander,G. and Guarente,L. (2004) The Sir2 family of protein deacetylases. *Annu. Rev. Biochem.*, **73**, 417–435.
31. Michan,S. and Sinclair,D. (2007) Sirtuins in mammals: insights into their biological function. *Biochem. J.*, **404**, 1–13.
32. Michishita,E., Park,J.Y., Burneskis,J.M., Barrett,J.C. and Horikawa,I. (2005) Evolutionarily conserved and nonconserved cellular localizations and functions of human SIRT proteins. *Mol. Biol. Cell.*, **16**, 4623–4635.
33. Vaquero,A., Scher,M.B., Lee,D.H., Sutton,A., Cheng,H.L., Alt,F.W., Serrano,L., Sternglanz,R. and Reinberg,D. (2006) SirT2 is a histone deacetylase with preference for histone H4 Lys 16 during mitosis. *Genes Dev.*, **20**, 1256–1261.
34. Brooks,C.L. and Gu,W. (2009) Anti-aging protein SIRT1: a role in cervical cancer? *Aging (Albany NY)*, **1**, 278–280.
35. Finkel,T., Deng,C.X. and Mostoslavsky,R. (2009) Recent progress in the biology and physiology of sirtuins. *Nature*, **460**, 587–591.
36. Crampton,A., Chang,F., Pappas,D.L. Jr, Frisch,R.L. and Weinreich,M. (2008) An ARS element inhibits DNA replication through a SIR2-dependent mechanism. *Mol. Cell*, **30**, 156–166.
37. Fox,C.A. and Weinreich,M. (2008) Beyond heterochromatin: SIR2 inhibits the initiation of DNA replication. *Cell Cycle*, **7**, 3330–3334.
38. Pappas,D.L. Jr, Frisch,R. and Weinreich,M. (2004) The NAD(+)-dependent Sir2p histone deacetylase is a negative regulator of chromosomal DNA replication. *Genes Dev.*, **18**, 769–781.
39. Zappulla,D.C., Sternglanz,R. and Leatherwood,J. (2002) Control of replication timing by a transcriptional silencer. *Curr. Biol.*, **12**, 869–875.
40. Douglas,N.L., Dozier,S.K. and Donato,J.J. (2005) Dual roles for Mcm10 in DNA replication initiation and silencing at the mating-type loci. *Mol. Biol. Rep.*, **32**, 197–204.
41. Liachko,I. and Tye,B.K. (2005) Mcm10 is required for the maintenance of transcriptional silencing in *Saccharomyces cerevisiae*. *Genetics*, **171**, 503–515.
42. Liachko,I. and Tye,B.K. (2009) Mcm10 mediates the interaction between DNA replication and silencing machineries. *Genetics*, **181**, 379–391.
43. Jeong,J., Juhn,K., Lee,H., Kim,S.H., Min,B.H., Lee,K.M., Cho,M.H., Park,G.H. and Lee,K.H. (2007) SIRT1 promotes DNA repair activity and deacetylation of Ku70. *Exp. Mol. Med.*, **39**, 8–13.
44. Li,K., Casta,A., Wang,R., Lozada,E., Fan,W., Kane,S., Ge,Q., Gu,W., Orren,D. and Luo,J. (2008) Regulation of WRN protein cellular localization and enzymatic activities by SIRT1-mediated deacetylation. *J. Biol. Chem.*, **283**, 7590–7598.
45. Matsuzaki,H., Daitoku,H., Hatta,M., Aoyama,H., Yoshimochi,K. and Fukamizu,A. (2005) Acetylation of Foxo1 alters its DNA-binding ability and sensitivity to phosphorylation. *Proc. Natl Acad. Sci. USA*, **102**, 11278–11283.
46. Vaziri,H., Dessain,S.K., Ng Eaton,E., Imai,S.I., Frye,R.A., Pandita,T.K., Guarente,L. and Weinberg,R.A. (2001) hSIR2(SIRT1) functions as an NAD-dependent p53 deacetylase. *Cell*, **107**, 149–159.
47. Yuan,Z., Zhang,X., Sengupta,N., Lane,W.S. and Seto,E. (2007) SIRT1 regulates the function of the Nijmegen breakage syndrome protein. *Mol. Cell*, **27**, 149–162.
48. Fan,W. and Luo,J. (2010) SIRT1 regulates UV-induced DNA repair through deacetylating XPA. *Mol. Cell*, **39**, 247–258.
49. Chen,L.F., Mu,Y. and Greene,W.C. (2002) Acetylation of RelA at discrete sites regulates distinct nuclear functions of NF-kappaB. *EMBO J.*, **21**, 6539–6548.
50. North,B.J., Marshall,B.L., Borra,M.T., Denu,J.M. and Verdin,E. (2003) The human Sir2 ortholog, SIRT2, is an NAD+-dependent tubulin deacetylase. *Mol. Cell*, **11**, 437–444.
51. Conti,C., Seiler,J.A. and Pommier,Y. (2007) The mammalian DNA replication elongation checkpoint: implication of Chk1 and relationship with origin firing as determined by single DNA molecule and single cell analyses. *Cell Cycle*, **6**, 2760–2767.
52. Conti,C., Leo,E., Eichler,G.S., Sordet,O., Martin,M.M., Fan,A., Aladjem,M.I. and Pommier,Y. (2010) Inhibition of histone deacetylase in cancer cells slows down replication forks, activates dormant origins, and induces DNA damage. *Cancer Res.*, **70**, 4470–4480.
53. Wong,S. and Weber,J.D. (2007) Deacetylation of the retinoblastoma tumour suppressor protein by SIRT1. *Biochem. J.*, **407**, 451–460.
54. Shevchenko,A., Tomas,H., Havlis,J., Olsen,J.V. and Mann,M. (2006) In-gel digestion for mass spectrometric characterization of proteins and proteomes. *Nat. Protoc.*, **1**, 2856–2860.
55. Liszt,G., Ford,E., Kurtev,M. and Guarente,L. (2005) Mouse Sir2 homolog SIRT6 is a nuclear ADP-ribosyltransferase. *J. Biol. Chem.*, **280**, 21313–21320.
56. Bonner,W.M., Redon,C.E., Dickey,J.S., Nakamura,A.J., Sedelnikova,O.A., Solier,S. and Pommier,Y. (2008) GammaH2AX and cancer. *Nat. Rev. Cancer*, **8**, 957–967.
57. Anglana,M., Apiou,F., Bensimon,A. and Debatisse,M. (2003) Dynamics of DNA replication in mammalian somatic cells: nucleotide pool modulates origin choice and interorigin spacing. *Cell*, **114**, 385–394.
58. Courbet,S., Gay,S., Arnoult,N., Wronka,G., Anglana,M., Brison,O. and Debatisse,M. (2008) Replication fork movement sets chromatin loop size and origin choice in mammalian cells. *Nature*, **455**, 557–560.
59. Yang,X.J. (2004) Lysine acetylation and the bromodomain: a new partnership for signaling. *Bioessays*, **26**, 1076–1087.
60. Li,A., Xue,Y., Jin,C., Wang,M. and Yao,X. (2006) Prediction of N_{ε}-acetylation on internal lysines implemented in Bayesian Discriminant Method. *Biochem. Biophys. Res. Commun.*, **350**, 818–824.

61. Sharma,A., Kaur,M., Kar,A., Ranade,S.M. and Saxena,S. (2010) Ultraviolet radiation stress triggers the down-regulation of essential replication factor Mcm10. *J. Biol. Chem.*, **285**, 8352–8362.
62. Kaur,M., Sharma,A., Khan,M., Kar,A. and Saxena,S. (2010) Mcm10 proteolysis initiates before the onset of M-phase. *BMC Cell Biol.*, **11**, 84.
63. Gay,S., Lachages,A.M., Millot,G.A., Courbet,S., Letessier,A., Debatisse,M. and Brison,O. (2010) Nucleotide supply, not local histone acetylation, sets replication origin usage in transcribed regions. *EMBO Rep.*, **11**, 698–704.
64. Iizuka,M. and Smith,M.M. (2003) Functional consequences of histone modifications. *Curr. Opin. Genet. Dev.*, **13**, 154–160.
65. Iizuka,M. and Stillman,B. (1999) Histone acetyltransferase HBO1 interacts with the ORC1 subunit of the human initiator protein. *J. Biol. Chem.*, **274**, 23027–23034.
66. Miotto,B. and Struhl,K. (2010) HBO1 histone acetylase activity is essential for DNA replication licensing and inhibited by Geminin. *Mol. Cell*, **37**, 57–66.
67. Terret,M.E., Sherwood,R., Rahman,S., Qin,J. and Jallepalli,P.V. (2009) Cohesin acetylation speeds the replication fork. *Nature*, **462**, 231–234.
68. Glozak,M.A. and Seto,E. (2009) Acetylation/deacetylation modulates the stability of DNA replication licensing factor Cdt1. *J. Biol. Chem.*, **284**, 11446–11453.
69. Paolinelli,R., Mendoza-Maldonado,R., Cereseto,A. and Giacca,M. (2009) Acetylation by GCN5 regulates CDC6 phosphorylation in the S phase of the cell cycle. *Nat. Struct. Mol. Biol.*, **16**, 412–420.
70. Balakrishnan,L., Stewart,J., Polaczek,P., Campbell,J.L. and Bambara,R.A. (2010) Acetylation of Dna2 endonuclease/helicase and flap endonuclease 1 by p300 promotes DNA stability by creating long flap intermediates. *J. Biol. Chem.*, **285**, 4398–4404.
71. Woodward,A.M., Göhler,T., Luciani,M.G., Oehlmann,M., Ge,X., Gartner,A., Jackson,D.A. and Blow,J.J. (2006) Excess Mcm2-7 license dormant origins of replication that can be used under conditions of replicative stress. *J. Cell Biol.*, **173**, 673–683.
72. Ge,X.Q., Jackson,D.A. and Blow,J.J. (2007) Dormant origins licensed by excess Mcm2-7 are required for human cells to survive replicative stress. *Genes Dev.*, **21**, 3331–3341.
73. Gilbert,D.M. (2007) Replication origin plasticity, Taylor-made: inhibition vs recruitment of origins under conditions of replication stress. *Chromosoma*, **116**, 341–347.
74. Ibarra,A., Schwob,E. and Méndez,J. (2008) Excess MCM proteins protect human cells from replicative stress by licensing backup origins of replication. *Proc. Natl. Acad. Sci. USA*, **105**, 8956–8961.
75. van Deursen,F., Sengupta,S., De Piccoli,G., Sanchez-Diaz,A. and Labib,K. (2012) Mcm10 associates with the loaded DNA helicase at replication origins and defines a novel step in its activation. *EMBO J.*, **31**, 2195–2206.
76. Kanke,M., Kodama,Y., Takahashi,T.S., Nakagawa,T. and Masukata,H. (2012) Mcm10 plays an essential role in origin DNA unwinding after loading of the CMG components. *EMBO J.*, **31**, 2182–2194.
77. Watase,G., Takisawa,H. and Kanemaki,M.T. (2012) Mcm10 plays a role in functioning of the eukaryotic replicative DNA helicase, Cdc45-Mcm-GINS. *Curr. Biol.*, **22**, 343–349.